A Full Dimensional Quasiclassical Trajectory Study of Cl + CH_4 Rate Coefficients†

Ernesto Garcia, Carlos Sánchez, Amaia Saracibar, and Antonio Laganà*

Departamento de Química Física, Universidad del País Vasco, 01006 Vitoria, Spain

Received: February 25, 2004; In Final Form: May 21, 2004

The Cl + CH_4 reaction has been investigated using a full dimensional quasiclassical trajectory technique and a new potential energy surface. The new surface is generated by expanding the interaction in terms of minimum energy paths in the Bond Order space. Results are compared with those obtained on another recently proposed potential energy surface and with experimental data.

1. Introduction

The study of the Cl + $CH_4 \rightarrow$ HCl + CH_3 reaction is of key importance for the modeling of atmospheric and combustion chemistry. In the stratosphere, at low temperatures (200−300 K), the reaction of CH_4 with Cl to produce HCl competes with that of O_3. Therefore, the Cl + CH_4 reaction acts as an important sink of the Cl atoms, and the determination of the rate coefficient of the Cl + CH_4 reaction plays a key role in modeling the depletion of the stratospheric ozone layer.[1,2] In combustion, at high temperatures (1000−2500 K), the Cl + CH_4 reaction significantly affects the outcome of clorohydrocarbons oxidations. Therefore, the determination of the rate coefficient of the Cl + CH_4 reaction is also important to model flames and determine their impact on the environment.[3]

This has prompted experimental studies of the Cl + CH_4 reaction aimed at determining the value of its thermal rate coefficient in the interval of temperatures T ranging from $T = 180$ to $T = 1100$ K. (At higher and lower temperatures experimental measurements are difficult to perform.) The measured rate coefficients exhibit a strong non-Arrhenius behavior. Measured values have been recently reviewed by the IUPAC Subcommittee on Gas Kinetics Data Evaluation for Atmospheric Chemistry. A value of $k = 1.0 \times 10^{-13}$ cm^3 $molecule^{-1}$ s^{-1} has been recommended for a temperature of 298 K.[4] Outside the interval of temperature covered by the experiment extrapolations have been provided in refs 5 and 6. Kinetic isotopic effects have also been studied. In particular, several measurements in which CH_4 has been substituted by CD_4 have been performed.[7−11] These measurements indicate that at high temperatures the reactivity of the deuterated methane is smaller by a factor of 2 than that of CH_4 and becomes more than 1 order of magnitude smaller at low temperatures.

In recent times a great deal of work has been performed to determine the potential energy surface (PES) of the Cl + CH_4 reaction. Accurate ab initio calculations have been performed by several authors.[12−18] Low level (HF/6-31G) ab initio calculations have been recently used in an on-the-fly trajectory study.[19] A full six-atom model PES, allowing the exchange of one hydrogen atom, was worked out (see ref 20) as a sum of four three-body LEPS functions (one for each Cl−H−C group of three atoms) plus a harmonic force field to describe the bending of the C−H bonds. Nyman and Yu proposed a semiempirical PES[21] assembled by summing a LEPS function for the Cl−H−C triatom to the CH_4 potential of Hase et al.[22,23] González et al. fitted the calculated ab initio points using a triatomic analytical functional of the many-body expansion (MBE)[24] type treating the CH_3 group as a pseudoatom.[18]

Corchado, Truhlar, and Espinosa-García[25] also fitted the ab initio values using an analytical PES consisting (like in the method proposed by Jordan and Gilbert for the H + CH_4 reaction[26]) of four LEPS functions (one for each Cl−H−C triatom) plus valence and out-of-plane bending terms. We shall refer to this potential as CTE.[17] The CTE PES allows the permutational symmetry of the hydrogen atoms by releasing a constraint embodied into a surface previously proposed by the same authors.[25] The CTE PES was used for transition state theory (TST) calculations obtaining a satisfactory reproduction of measured rate coefficients and kinetic isotopic effects.[17] On the CTE PES we have carried out extended quasiclassical trajectory (QCT) calculations to investigate whether a full dimensional trajectory study would confirm the positive conclusions of the TST investigation. The results of this investigation have motivated the assemblage of a new PES and new QCT calculations.

Accordingly, this paper is organized as follows: In Section 2 the results of a QCT study performed on the CTE PES are illustrated. In Section 3 a new potential energy surface of the Minimum Energy Path − Many Process Expansion (MEP-MPE) type[27] based on Bond Order (BO) coordinates is proposed, and the results of a QCT study performed on it are discussed. In Section 4, the kinetic isotopic effect obtained by substituting CH_4 with CD_4 is analyzed for both the CTE and the MEP-MPE PESs.

2. The QCT Calculations on the CTE PES

As already mentioned, we first performed extended QCT calculations on the CTE[17] potential energy surface to compare full dynamical and TST results.

2.1. The CTE PES. The CTE PES for Cl + CH_4 is assembled out of four stretching and two bending terms: $V^{CTE} = V_{str} + V_{val} + V_{op}$. The stretching terms V_{str} account for the deformation of the Cl−H−C bonds and are formulated as LEPS potentials. The bending term V_{val} accounts for the in plane motion and is formulated as a sum of the harmonic contributions associated with the in plane displacement from equilibrium.[26] The other bending term V_{op} accounts for the out of plane motion and is

† Part of the "Gert D. Billing Memorial Issue".

* Permanent address: Dipartimento di Chimica, Università di Perugia, 06123 Perugia, Italy.

10.1021/jp049154h CCC: $27.50
Published on Web 08/11/2004

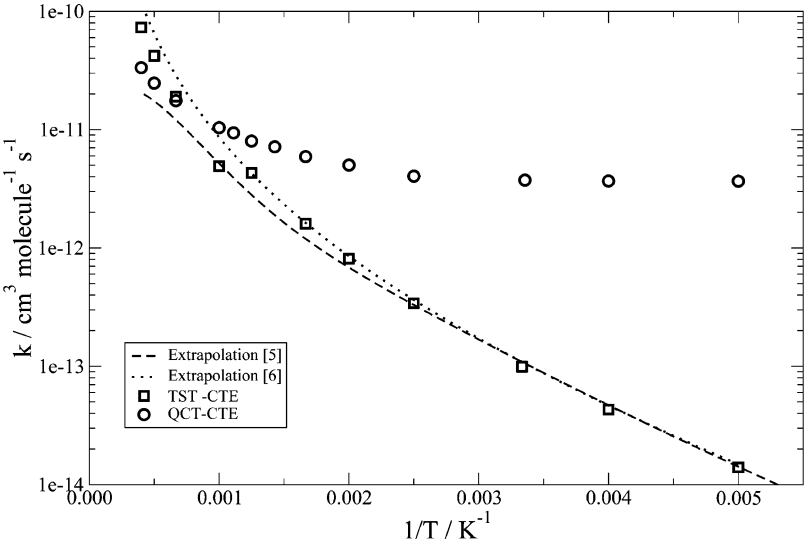

Figure 1. TST (open squares) and QCT (open circles) rate coefficients for the CTE PES. For comparison, two different interpolation curves (dashed line[5] and dotted line[6]) of the experimental values are also shown.

formulated as a sum of the second and fourth order terms of the expansion in the displacement from equilibrium.[26]

The parameters of the CTE PES were optimized to reproduce the equilibrium geometries as well as the frequencies and the energies of the reactants, of the products, and of the transition state. The optimization has also taken into account the dependence of the thermal rate coefficient on the temperature and of the room-temperature isotopic ratio. The CTE PES is endoergic of 6.1 kcal/mol, has a saddle to reaction 7.7 kcal/mol higher than the reactant asymptote, and shows two wells (absent from the ab initio data). One well is located inside the entrance channel and is 3.2 kcal/mol deeper than the reactant asymptote, while the other well is located inside the product channel (4.7 kcal/mol deeper than the product asymptote).

2.2. The QCT Calculations. On the CTE PES we carried out rate coefficient calculations at several temperature values falling in the range 200−2500 K. At each temperature the number of calculated trajectories was chosen large enough to make the statistical error lower than 5% (At $T = 200$ K more than 120000 trajectories were integrated, while at $T = 1000$ K 60000 trajectories were found to be sufficient.). Particular care was put on the calculations of the rate coefficient performed at $T = 298$ K for which more than half a million trajectories were integrated reducing the statistical error to less than 1.5%. The calculated rates were multiplied by a factor 1/3 to account for the fact that out of the three surfaces ($1\ ^2A'$, $2\ ^2A'$, and $1\ ^2A''$) involved in the $Cl(^2P) + CH_4(X\ ^1A_1)$ reaction only the $1\ ^2A'$ correlates adiabatically with the products $HCl(X\ ^1\Sigma_1^+) + CH_3(X\ ^2A_2'')$.

The calculations were carried out using a version of VENUS96[28] customized to incorporate the CTE PES and its analytic derivatives. The input parameters of the program were chosen to be the following: the integration step 0.1 fs, the initial and final separations of the collision fragments 8.5 Å, and the maximum impact parameter 8.0 Å. The vibrational energy of the reactant CH_4 molecule was set to correspond to that of the ground state calculated using a normal coordinate approach (This can lead to a slight underestimate of the value of the rate coefficients at the higher temperatures considered here.). The rotational energy was set equal to $k_BT/2$ (with k_B being, as usual, the Boltzmann constant) around each principal axis of inertia. The translational energy was randomly selected to mimic the Boltzmann distribution for the chosen temperature. The values of the remaining parameters were selected randomly.

It has to be emphasized here that both reactant (initial) and product (final) separations need to be large enough to make the interaction between the separated fragments sufficiently small (In our calculations we set this distance to be 8.5 Å so as to have, on the average, an interaction energy between the two reactant fragments of 0.07 kcal/mol.). The impact parameter was also taken large enough (up to 8.0 Å) to include all the significant contributions to reaction.

2.3. The Rate Coefficients. The QCT rate coefficients for the reaction Cl + CH_4 calculated on the CTE PES are shown in Figure 1 (open circles). In the same figure the corresponding values obtained by Corchado et al.[17] using the *canonical unified statistical model with optimized multidimensional tunneling* approach (CUS/μOMT) version of the TST method are shown as open squares. Both sets of calculated values are compared in the figure with the two curves (dashed line from ref 5 and dotted line from ref 6) interpolated from the experiment.

As apparent from the figure, the temperature dependence of the thermal rate coefficient obtained on the CTE PES from the transition state theory well reproduces that of the most recent fit to the measured data. On the contrary, the full dimensional QCT estimates of the rate coefficient calculated on the same PES deviate significantly from it. The discrepancy is large at both high and low temperature. It varies from a factor 2 at high temperature to more than 2 orders of magnitude at low temperature. This means that part of the agreement of TST calculations with the experiment is due to their reduced dimensionality.

3. The MEP-MPE PES and Related Calculations

To obtain a better reproduction of the measured rate coefficients using a full dimensional QCT approach we investigated the possibility of building a new PES (the already mentioned MEP-MPE, Minimum Energy Path − Many Process Expansion PES[27,29]) inspired to the scheme proposed by Ochoa and Clary[30] who generalized to polyatomic reactions the concept of many process expansion (MPE) approaches.[31−37]

3.1. The Bond Order MPE Formulation of the Interaction. A key problem of the functional representation of the interaction is the fact that direct or inverse powers of physical coordinates are unsuitable to formulate the interaction of neutral molecules over the entire range of distances.

To overcome this difficulty it has been suggested to use BO coordinates.[38] These coordinates are quite suitable for this

purpose since they have built-in the metrics of molecular bonds. They become, in fact, large at short distances, one at the atom−atom equilibrium distance, and zero at infinity. The BO coordinate for the generic $\kappa\lambda$ pair of atoms is defined as

$$n_{\kappa\lambda} = \exp[-\beta_{\kappa\lambda}(r_{\kappa\lambda} - r_{e\kappa\lambda})] \quad (1)$$

with $r_{\kappa\lambda}$ being the internuclear distance, $r_{e\kappa\lambda}$ being the corresponding equilibrium value, and $\beta_{\kappa\lambda}$ being a parameter related to the bond strength of the $\kappa\lambda$ diatom.

The diatomic (two-body) potential ($V^{(2)}$) of the diatom $\kappa\lambda$ can be expressed in the bond order formalism as a polynomial of the related BO variable[38]

$$V^{(2)}(r_{\kappa\lambda}) = -D_{e\kappa\lambda}\sum_{j=1}^{G} a_{\kappa\lambda,j} n_{\kappa\lambda}^{j} \quad (2)$$

with G being the power of the polynomial and $D_{e\kappa\lambda}$ being the diatomic dissociation energy. Then the $\beta_{\kappa\lambda}$ parameter and the $a_{\kappa\lambda,j}$ coefficients are obtained by best fitting either the ab initio electronic energies or the spectroscopic data.

For polyatomic systems a popular approach is the Many Body Expansion (MBE) one suggested by Murrell and collaborators.[24] In the MBE approach the potential is expanded in interactions of an increasing numbers of atoms:

$$V = V^{(2)} + V^{(3)} + V^{(4)} + ... \quad (3)$$

In the case of three atom systems (say $\kappa\lambda\mu$) the only additional many body term is the three-body one that reads

$$V^{(3)}(r_{\kappa\lambda}, r_{\lambda\mu}, r_{\mu\kappa}) = \sum_{\substack{i+j+k\neq i\neq j\neq k \\ i+j+k\leq H}}^{H} c_{\kappa\lambda\mu,ijk}\, n_{\kappa\lambda}^{i}\, n_{\lambda\mu}^{j}\, n_{\mu\kappa}^{k} \quad (4)$$

where the summation, as specified in ref 39, is over all crossed terms (excluding single variable ones) up to an overall order H. Sometimes, also the RBO variables given by the product of the BO coordinates for the related internuclear distances[40,41] are used. Accordingly, the three-body term has the form

$$V^{(3)}(r_{\kappa\lambda}, r_{\lambda\mu}, r_{\mu\kappa}) = \sum_{\substack{i+j+k\neq i\neq j\neq k \\ i+j+k\leq H}}^{H} c_{\lambda\mu\nu,\,ijk}(r_{\kappa\lambda}n_{\kappa\lambda})^{i}(r_{\lambda\mu}n_{\lambda\mu})^{j}(r_{\mu\kappa}n_{\mu\kappa})^{k} \quad (5)$$

Both formulations have been used to fit the PES of three atom systems.[39−48] Extensions to four and five atom systems have also been reported.[49−52]

A simple way of formulating the PES as a BO polynomial suitable for a straightforward generalization to polyatomic systems is the ALBO one in which the overall potential is formulated in the following pseudopair additive form[27,53]

$$V(\{n\}) = \sum_{j} D_j(1 + Q_j(\{n_k\}_{k\neq j}))P_j(n_j) \quad (6)$$

where j and k run over all diatomic pairs making the functional a sum of pseudo ("effective") diatomic model potentials having a shape depending on the proximity of the other atoms. For this reason, Q_j and P_j are expressed as (low order) polynomials in the BO variables. In particular, Q_j depends on all the BO variables but n_j and makes the depth of the effective diatomic potential depend on the vicinity of the other atoms. Due to the nature of the BO variables these contributions vanish when the other atoms fly away. P_j depends explicitly only on n_j; yet its coefficients too depend parametrically on the other n_k variables.

To generalize the BO formulation of the PES to large systems we followed here the alternative MPE approach. In the MPE scheme given the set of atoms $\kappa\lambda\mu\nu$... one can formulate the PES as a sum of all the possible processes ξ connecting reactants to products

$$V_{\kappa\lambda\mu\nu...} = \sum_{\xi} W_{\xi}(\mathbf{s}_{\xi})\, V_{\xi}(\mathbf{t}_{\xi}) \quad (7)$$

where $\mathbf{s}_{\xi}$ is the evolution coordinate (or reaction coordinate) of process ξ driving the transformation of the system from reactants to products, while $\mathbf{t}_{\xi}$ is the set of coordinates describing the local deformation of the system. In eq 7 $V_{\xi}(\mathbf{t}_{\xi})$ is the functional describing the cut of the reaction channel at each point of the evolution coordinate, while $W_{\xi}(\mathbf{s}_{\xi})$ is a weight function that properly averages the contributions coming from different processes. In this way the permutational symmetry of the system is fully taken into account.

A suitable evolution coordinate can be defined using the polar representation of the BO coordinates (Hyperspherical Bond Order or HYBO coordinates[54,55]). As an example, for three atom systems and the specific $\xi = \kappa\lambda\mu$ (i.e. $\kappa + \lambda\mu \rightarrow \kappa\lambda + \mu$) process the evolution coordinate $\alpha_{\kappa\lambda\mu}$ can be expressed[32−34] as

$$\alpha_{\kappa\lambda\mu} = \arctan\left(\frac{n_{\lambda\mu}}{n_{\kappa\lambda}}\right) \quad (8)$$

where $n_{\kappa\lambda}$ and $n_{\lambda\mu}$ are the relevant BO coordinates and $\alpha_{\kappa\lambda\mu}$ can be understood as the angle of rotation from the initial diatom $\lambda\mu$ to the final diatom $\kappa\lambda$ (from this the name ROtating Bond Order or ROBO potential). The corresponding collective coordinate that accounts for the stretching of the system while it evolves from reactants to products is the hyperradius $\rho_{\kappa\lambda\mu}$ defined as

$$\rho_{\kappa\lambda\mu} = \sqrt{n_{\kappa\lambda}^2 + n_{\lambda\mu}^2} \quad (9)$$

Similarly for the four atom $\kappa\lambda\mu\nu$ (i.e. $\kappa\lambda + \mu\nu \rightarrow \kappa + \lambda\mu\nu$) process one has an angle $\alpha_{\kappa\lambda\mu\nu}$ defined as

$$\alpha_{\kappa\lambda\mu\nu} = \arctan\left(\frac{n_{\mu\nu}}{n_{\kappa\lambda}}\right) \quad (10)$$

and hyperradius $\rho_{\kappa\lambda\mu\nu}$ defined as

$$\rho_{\kappa\lambda\mu\nu} = \sqrt{n_{\kappa\lambda}^2 + n_{\lambda\mu}^2 + n_{\mu\nu}^2} \quad (11)$$

In this case, however, four additional angles need to be defined.[35−37]

This type of Many Process Expansion has been used to assemble the PES of some three[33,34,56−58] and four[35,36,37,59] atom reactions.

3.2. The MEP-MPE Formulation of the Interaction. When moving to larger systems the explicit consideration of all the possible processes of a pure MPE approach becomes quite demanding. After all, in general, the key information for the calculation of the low energy dynamics of reactive systems is that associated with the portion(s) of the PES located in the proximity of the minimum energy path or paths. For this reason one can express the relevant processes in terms of the MEP segments connecting reactants to products through all possible types of transition states or stable intermediates (stationary points). Moreover, the complexity of the treatment can be further

reduced by discarding from the expansion of eq 7 the processes involving paths falling outside (above) the energy range of interest. Finally, each point of the considered sections of V_ξ is formulated as a sum of two terms: the term $V_{\xi,\mathrm{mep}}$ associated with the minimum energy path closer to the considered arrangement and the terms $V_{\xi,\mathrm{mbe}}$ associated with the correction for the deviation of the geometry considered from the nearest minimum energy configuration:

$$V_\xi = V_{\xi,\mathrm{mep}} + V_{\xi,\mathrm{mbe}} \tag{12}$$

The correction term $V_{\xi,\mathrm{mbe}}$ is then further articulated into two- (2), three- (3), and four- (4) body components such as in the usual MBE approach

$$V_{\xi,\mathrm{mbe}} = \sum_i V^{(2)}_{i\xi,\mathrm{mbe}} + \sum_i V^{(3)}_{i\xi,\mathrm{mbe}} + \sum_i V^{(4)}_{i\xi,\mathrm{mbe}} \tag{13}$$

where the index i runs over all the two, three, and four sets of atoms. The two-body components read

$$V^{(2)}_{i\xi,\mathrm{mbe}} = D^{(2)}_{i\xi,\mathrm{mbe}}\,(n_i - n_{i\xi,\mathrm{mep}})^2 \tag{14}$$

to account for the difference between the related BO coordinate n_i and its reference value $n_{i\xi,\mathrm{mep}}$ taken at the corresponding point on the nearest minimum energy path. It is worth noting here that the two-body expression of eq 14 is anharmonic in the physical space despite its harmonic-like formulation in the BO space. The three-body components read

$$V^{(3)}_{i\xi,\mathrm{mbe}} = D^{(3)}_{i\xi,\mathrm{mbe}}\,(\phi_{i\xi} - \phi_{i\xi,\mathrm{mep}})^2 \tag{15}$$

to account for the difference between the related actual bending angle $\phi_{i\xi}$ and that of the corresponding geometry on the nearest minimum energy path $\phi_{i\xi,\mathrm{mep}}$. The four-body components read

$$V^{(4)}_{i\xi,\mathrm{mbe}} = D^{(4)}_{i\xi,\mathrm{mbe}}\,(\zeta_{i\xi} - \zeta_{i\xi,\mathrm{mep}})^2 \tag{16}$$

to account for the difference between the related actual torsion angle $\zeta_{i\xi}$ and that of the corresponding geometry on the nearest minimum energy path $\zeta_{i\xi,\mathrm{mep}}$.

Finally the weight function W_ξ is expressed as a normalized sum of the individual process weights w_ξ defined as

$$w_\xi = \prod_j \exp[-b(n_j - n_{j\xi,\mathrm{mep}})^2] \tag{17}$$

where the product extends over all the j pairs of atoms of the system and the parameter b controls the width of the Gaussian.

3.3. The MEP-MPE PES for the Cl + CH_4 Reaction. The MEP-MPE PES for the Cl + CH_4 → HCl + CH_3 reaction has been worked out by considering that there is a single MEP connecting both reactant (R) and product (P) asymptotes to the saddle point (S) as singled out by the ab initio calculations of ref 12. The reactant arrangement consists of the isolated Cl atom and the CH_4 molecule. At the reactive saddle a C−H bond (of CH_4) is weakened (its length is stretched) to allow one of the four hydrogen atoms (hereafter labeled as H1) to interact with Cl and form a collinear-like C−H1−Cl intermediate. The other three C−H bonds are symmetrically arranged around the C−H1−Cl axis (symmetry C_{3v}). The product arrangement consists of the isolated HCl and CH_3 molecules.

Accordingly, the MEP was partitioned into two V_ξ segments. The first segment goes from reactants to the saddle, while the second segment goes from the saddle to products. The MEP energy of each segment was then calculated using a third degree polynomial to interpolate the ab initio potential energy value of the extrema of the interval while satisfying the continuity condition for its derivative. Similarly the corrective contributions were evaluated by interpolating the D parameters of eqs 14, 15, and 16 from their values at the R, P, or S extrema of the relevant interval.

The $D^{(2)\mathrm{X}}_{\mathrm{mbe}}$ (X≡R,P,S) values used to fit the various $D^{(2)}_{i\xi,\mathrm{mbe}}$ parameters were essentially the dissociation energies of the isolated diatoms (78.3, 106.4, 78.2, 109.5 kcal/mol for, respectively, Cl−C, Cl−H, C−H, and H−H). For the reactant geometry the $D^{(2)\mathrm{R}}_{\mathrm{mbe}}$ value of C−H was multiplied by a factor of 0.93. For the saddle geometry, the $D^{(2)\mathrm{S}}_{\mathrm{mbe}}$ value of Cl−H1 and C−H1 was set at 60.0 kcal/mol to take into account the relaxation of both the Cl−H1 bond of the HCl product and the C−H1 bond of the CH_4 reactant. No changes were introduced for the products.

The three-body correction term includes only the most important contributions. In fact, for the reactant geometry only the contribution due to the H−C−H bending motion of the CH_4 molecule was considered (the value of the related $D^{(3)\mathrm{R}}_{\mathrm{mbe}}$ parameter was set at 34 kcal/mol), while for the product geometry only the H−C−H bending motion of the CH_3 molecule was considered (the value of the related $D^{(3)\mathrm{P}}_{\mathrm{mbe}}$ parameter was set at 14 kcal/mol, by making the molecule much floppier than CH_4). At the saddle geometry, a distinction between the bending motion of H1−C−H and that of H−C−H was made. The value of the $D^{(3)\mathrm{S}}_{\mathrm{mbe}}$ parameter for H1−C−H was taken to be 35 kcal/mol, slightly higher than that of the CH_4 molecule but significantly higher than that of the CH_3 product molecule, while the value of the $D^{(3)\mathrm{S}}_{\mathrm{mbe}}$ parameter for H−C−H was taken to be less energetic (30 kcal/mol).

The $D^{(4)\mathrm{X}}_{\mathrm{mbe}}$ parameters of the four-body correction terms were assumed to be negligible. An exception is made for the product geometry where for the Cl−H1−C−H torsion a small correction of 0.4 kcal/mol is considered to take into account the loss of planarity of the CH_3 molecule.

The resulting MEP-MPE surface is endoergic of 6.7 kcal/mol and has a saddle point 7.9 kcal/mol higher than the reactant asymptote. No wells are located on the minimum energy path. The equilibrium geometries of the reactant and product molecules of the MEP-MPE PES are in excellent agreement with the spectroscopic data. The vibrational harmonic frequencies are in general quite well reproduced. The geometry of the saddle point of the MEP-MPE PES has a symmetry C_{3v} being the internuclear distances Cl−H1, H1−C, and C−H 1.431, 1.388, and 1.086 Å, respectively. The angles ∠(Cl−H1−C) and ∠(H1−C−H) are 180° and 101.4°, respectively. These geometrical data are in good agreement with the ab initio information. The harmonic frequencies of the saddle point of the MEP-MPE PES fall in general within the error bars of the ab initio values. The main difference is found in the imaginary frequency value that is underestimated in the MEP-MPE PES. All the other details of this first MEP-MPE PES are given in refs 27 and 29.

3.4. The QCT Calculations on the MEP-MPE PES. The thermal rate coefficient for the Cl + CH_4 reaction has been calculated in a wide interval of temperatures (200−2500 K) using the already mentioned modified version of VENUS96.[28] Yet, on the MEP-MPE PES the derivatives were calculated numerically (contrary to what was made for the CTE PES). For most of the other parameters and conditions the choice made for the MEP-MPE PES is similar to that made for the CTE PES. The most notable differences are those associated with

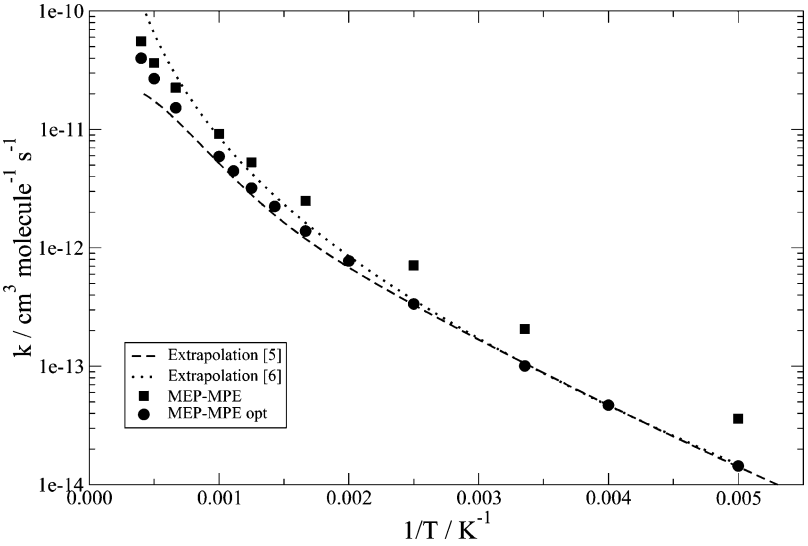

Figure 2. QCT rate coefficients calculate on the first (solid squares) and optimized (solid circles) MEP-MPE PESs. For comparison, two different interpolation curves (dashed line[5] and dotted line[6]) of the experimental values are also shown.

the maximum value of the impact parameter and with both the initial and final separations (that were significantly reduced). In fact, since the initial and final separations were set up at 5.0 Å, the interaction between the asymptotic fragments is as low as that of the CTE PES that uses the larger separation of 8.5 Å. Similarly, a maximum impact parameter of 3.0 Å is sufficient for collecting all the reactive contributions (in contrast with the larger value of 8.0 Å used for the CTE PES). The number of trajectories calculated at each temperature is large enough to lead to errors lower than 9% for the rate coefficients.

The key result obtained from the QCT calculation is the value of the rate coefficient at room temperature (298 K). This value is $k = 2.07 \pm 0.18 \times 10^{-13}$ cm^3 molecule^{-1} s^{-1} that is a factor of 2 higher than the IUPAC recommended value.[4] However, the dependence of the rate coefficient on the temperature obtained on the first MEP-MPE PES is in fairly good agreement with the experimental findings (solid squares in Figure 2).

To scale the rate coefficient values to the experimental data we played with the parameter $D_{mbe}^{(3)S}$ of the three-body correction term for the Cl−H1−C bending motion. This term controls the cone of acceptance of Cl when approaching CH_4. As a matter of fact, a null value of $D_{mbe}^{(3)S}$(Cl−H1−C), as that used for building up the first MEP-MPE PES, implies that the corresponding term of the three-body correction $V_{\xi,mbe}^{(3)}$ is zero for all values of the Cl−H1−C angle. On the contrary, when $D_{mbe}^{(3)S}$(Cl−H1−C) differs from zero, $V_{\xi,mbe}^{(3)}$ has a zero value in the case that the geometry of the system coincides with the reference configuration of the (collinear) transition state and increasingly becomes more positive (more repulsive) as the angle Cl−H1−C deviates from collinearity. Accordingly, when $D_{mbe}^{(3)S}$(Cl−H1−C) is zero, even for geometries sufficiently far from collinearity the potential energy is small enough to allow an abstraction of the hydrogen atom. Whereas as $D_{mbe}^{(3)S}$(Cl−H1−C) gets larger the interval of energetically favorable angles of attack increasingly narrows. To this end, the $D_{mbe}^{(3)S}$(Cl−H1−C) parameter was set equal to 0.7, 1.0, 1.5, 1.7, 2.0, and 2.5 kcal/mol to estimate the dependence of the room-temperature QCT rate coefficient calculated on the corresponding MEP-MPE PESs. For each value of $D_{mbe}^{(3)S}$(Cl−H1−C), we have integrated a number of trajectories large enough to keep the percentual error lower than 7%. The results obtained are shown in Figure 3. As apparent from the figure, an increase of

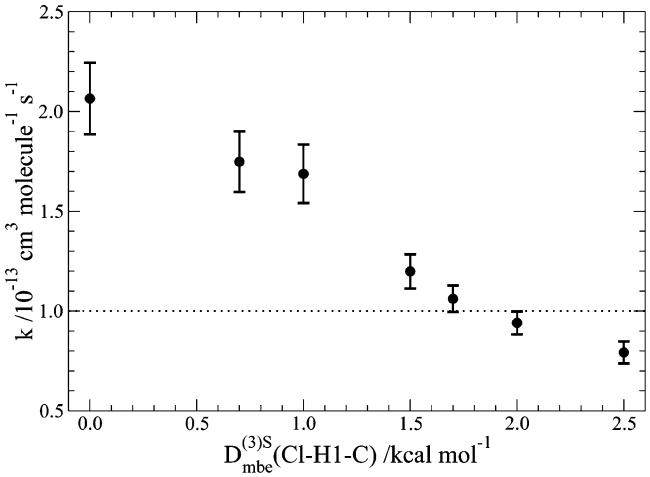

Figure 3. QCT rate coefficients at room-temperature calculated on several MEP-MPE PESs as a function of the $D_{mbe}^{(3)S}$(Cl−H1−C) parameter (see Section 3.3 of the text). The IUPAC recommended value is shown as a dotted line.[4]

the $D_{mbe}^{(3)S}$(Cl−H1−C) parameter decreases the rate coefficient. By interpolating over these results the appropiate value of $D_{mbe}^{(3)S}$(Cl−H1−C) was found to be 1.84 kcal/mol. On this optimized MEP-MPE surface, we have calculated the rate coefficient in the range of temperatures going from 200 to 2500 K. The large batches of integrated trajectories (for instance near 300000 at room temperature) kept the percentual error below 5%. The rate coefficients calculated using the optimized MEP-MPE PES are plotted in Figure 2 (solid circles) as a function of the temperature *T*. As apparent from the figure, the agreement of the calculated QCT rate coefficients with the experiment is particularly good at low temperature ($k = 1.01 \pm 0.04 \times 10^{-13}$ cm^3 molecule^{-1} s^{-1} at $T = 298$ K). At high temperature the calculated values lie, as expected, between the two curves extrapolated from experimental data.

4. Isotopic Effect

QCT calculations of the thermal rate coefficients were performed also for the Cl + CD_4 reaction. For this purpose both CTE and the optimized MEP-MPE PESs were used. In this way it was possible to estimate the kinetic isotopic effect (KIE) defined as the ratio k_{Cl+CH_4}/k_{Cl+CD_4} between the rate coefficient

TABLE 1: k_{Cl+CH_4}/k_{Cl+CD_4} Isotopic Effect Calculated Using QCT, TST, and LSC−IVR Techniques on Both the CTE and the Optimized MEP-MPE PESs[h]

	CTE			MEP-MPE	
T/K	TST[a]	IVR[b]	QCT	QCT	experiment
200	87.7		16.0 ± 1.2	31.3 ± 13.5	
298	14.3		12.0 ± 0.6	8.0 ± 0.9	10.7,[c] 13.6,[d] 16.4,[e] 12.2,[f] 18.5[g]
400	5.6	4.8	7.9 ± 0.8	4.8 ± 0.6	5.2,[c] 6.4[d]
500	3.3	3.0	7.0 ± 0.7	3.6 ± 0.4	4.1[d]
800	1.6	1.6	4.4 ± 0.4	2.6 ± 0.2	2.1[d]
1000	0.8	1.4	4.0 ± 0.3	2.1 ± 0.2	1.7[d]
2000	1.3	1.2	2.5 ± 0.2	1.7 ± 0.1	1.7[d]

[a] Reference 17. [b] Reference 61. [c] Reference 7. [d] Reference 8. [e] Reference 9. [f] Reference 10. [g] Reference 11. [h] For comparison, also the values obtained from the experiment are shown.

of Cl + CH_4 and that of Cl + CD_4 and compare the calculated KIE with the measured one for a wide range of temperatures (295−1018 K).[7−11]

For the Cl + CD_4 calculations the same parameters adopted for Cl + CH_4 were used. A larger number of trajectories (for example, more than 800000 at 298 K for the MPE-MPE PES) have been calculated to make the statistical error as small as 7% due to the low reactivity of the deuterated reaction.

The calculated KIEs are compared with the experiment in Table 1. In Table 1, also the values obtained on the CTE PES using the TST[17] and the linearized semiclassical-initial value representation (LSC−IVR[60])[61] are given.

As can be seen from Table 1, the values of KIE measured at room temperature are quite scattered making the comparison of theoretical results with the experiment quite difficult. The KIEs calculated on the CTE PES always fall within the experimental error bar regardless the technique used. However, their dependence on the temperature highly varies with the theoretical approach used. In fact, at 200 K the QCT KIE increases about 40% with respect to the room temperature one, while the corresponding TST KIE increases about 500%. On the contrary, as the temperature increases, the KIE decreases less for QCT results than for TST and LSC−IVR ones. Accordingly, at high temperature, the QCT approach overestimates the KIE, while the TST and the LSC−IVR ones underestimate it. Please note that at 1000 K the TST-CTE result predicts an inversion of the isotopic effect.

The KIE calculated on the optimized MEP-MPE PES at room temperature is smaller than the measured one. However, this underestimation is reduced as the temperature increases and at high temperatures the agreement is good. This may mean that quantum tunneling may be important at low temperature for Cl + CH_4 (and less important for Cl + CD_4). This may also mean that the MEP-MPE PES may need further refining work depending of the effect that the introduction of tunneling has on the efficiency of the reactive process. Unfortunately attempts to estimate this effect using a TST approach have not led to unique conclusions. The only way to draw valid conclusions on this is to assemble a specific quantum program for dealing with polyatomic reactions.

5. Conclusions

This paper reports on the work done to assemble a suitable PES for the Cl + CH_4 reaction and to test it using quasiclassical calculations (thermal rate coefficients and kinetic isotopic effects). Values calculated on a previously proposed CTE PES (leading to a satisfactory agreement with the experiment when using a transition state approach) deviate up to 2 orders of magnitude from measured data when using quasiclassical techniques. For this reason we turned our attention onto the MEP-MPE PES designed to fit in a piecewise way the potential energy paths connecting the stationary points of the surface. The assembled MEP-MPE PES has an endoergicity and a barrier similar to those of the CTE PES. The main difference between the two surfaces is the presence, in the CTE PES, of two deep wells located in the reactant and the product channels, respectively. These wells cannot be found in the MEP-MPE PES (as well as in ab initio data). This feature can explain the different results obtained with the two surfaces.

The QCT calculations have also shown that the MEP-MPE PES is not only accurate enough to lead to the reproduction of the measured temperature dependence of the thermal rate coefficient but also flexible enough to allow the anchoring of its theoretical value to the value measured at room temperature. To do this it has been sufficient to play with the value of the parameter of the bending component of the interaction at the transition state. This flexibility will allow for carrying out further refinements in order to obtain accurate estimates of the detailed dynamical properties. As an example, test calculations mimicking the conditions of an experiment of Zare and collaborators[62] showed that the rotational population of the HCl(v'=0) and HCl(v'=1) products of the reaction Cl + CH_4(v=1) → HCl(v',j') + CH_3 are hotter than the measured ones. We are planning, however, to carry out this finer tuning together with a full dynamical quantum calculation.

Acknowledgment. Financial support from MCyT, MIUR, ASI, and COST in Chemistry is acknowledged. Thanks are due to the authors of ref 17 who sent us their potential energy surface routine.

References and Notes

(1) Wayne, R. P. *Chemistry of Atmospheres*, 3rd ed.; Oxford University Press: Oxford, 2000.
(2) Michelsen, H. A.; Salawitch, R. J.; Gunson, M. R.; Aellig, C.; Kämpfer, N.; Abbas, M. M.; Abrams, M. C.; Brown, T. L.; Chang, A. Y.; Goldman, A.; Irion, F. W.; Newchurch, M. J.; Rinsland, C. P.; Stiller, G. P.; Zander, R. *Geophys. Res. Lett.* **1996**, *23*, 2361.
(3) Senkan, S. M.; Robinson, J. M.; Gupta, A. K. *Combust. Flame* **1983**, *49*, 305.
(4) Atkinson, R.; Baulch, D. L.; Cox, R. A.; Hampson, R. F.; Kerr, J. A.; Rossi, M. J.; Troe, J. *J. Phys. Chem. Ref. Data* **1999**, *28*, 191.
(5) Michelsen, H. A.; Simpson, W. R. *J. Phys. Chem. A* **2001**, *105*, 1476.
(6) Bryukov, M. G.; Slagle, I. R.; Knyazev, V. D. *J. Phys. Chem. A* **2002**, *106*, 10532.
(7) Chilts, G.; Eckling, R.; Goldfinger, P.; Huybretchts, G.; Johnston, H. S.; Meyers, L.; Verbeke, G. *J. Chem. Phys.* **1963**, *38*, 1053.
(8) Clyne, M. A. A.; Walker, R. F. *J. Chem. Soc., Faraday Trans. 1* **1973**, *169*, 1547.
(9) Wallington, T. J.; Hurley, M. D. *Chem. Phys. Lett.* **1992**, *189*, 437.
(10) Matsumi, Y.; Izumi, K.; Skorokhodov, V.; Kawasaki, M.; Tanaka, N. *J. Chem. Phys.* **1997**, *101*, 1216.
(11) Boone, G. D.; Agyin, F.; Robichaud, D. J.; Tao, F.-M.; Hewitt, S. A. *J. Phys. Chem. A* **2001**, *105*, 1456.
(12) Truong, T. N.; Truhlar, D. G.; Baldridge, K. K.; Gordon, M. S.; Steckler, R. *J. Chem. Phys.* **1989**, *90*, 7137.
(13) Dobbs, K. D.; Dixon, D. A. *J. Phys. Chem.* **1994**, *98*, 12584.
(14) Duncan, W. T.; Truong, T. N. *J. Chem. Phys.* **1995**, *103*, 9642.
(15) Roberto-Neto, O.; Coitiño, E. L.; Truhlar, D. G. *J. Phys. Chem. A* **1998**, *102*, 4568.
(16) Hu, H.-G.; Nyman, G. *J. Chem. Phys.* **1999**, *111*, 6693.
(17) Corchado, J. C.; Truhlar, D. G.; Espinosa-Garcia, J. *J. Chem. Phys.* **2000**, *112*, 9375.
(18) Troya, D.; Millán, J.; Baños, I.; González, M. *J. Chem. Phys.* **2002**, *117*, 5730.
(19) Rudic, S.; Murray, C.; Harvey, J. N.; Orr-Ewing, A. *J. Chem. Phys.* **2004**, *120*, 186.
(20) Wang, X.; Ben-Nun, M.; Levine, R. D. *Chem. Phys.* **1995**, *197*, 1.
(21) Yu, H.-G.; Nyman, G. *Phys. Chem. Chem. Phys.* **1999**, *1*, 1181.

(22) Hase, W. H.; Mondro, S. L.; Duckovic, R. J.; Hirst, D. M. *J. Am. Chem. Soc.* **1984**, *109*, 2916.
(23) Duckovic, R. J.; Hase, W. H.; Schlegel, H. B. *J. Phys. Chem.* **1984**, *88*, 1339.
(24) Murrell, J. N.; Carter, S.; Farantos, S. C.; Huxley, P.; Varandas, A. J. C. *Molecular Potential Energy Surfaces*; Wiley: New York, 1984.
(25) Espinosa-Garcia, J.; Corchado, J. C. *J. Chem. Phys.* **1996**, *105*, 3517.
(26) Jordan, M. J. T.; Gilbert, J. *J. Chem. Phys.* **1995**, *102*, 5669.
(27) Garcia, E.; Sánchez, C.; Albertì, M.; Laganà, A. *Lect. Notes Comput. Sci.* **2004**, *3044*, 328.
(28) Hase, W. L.; Duchovic, R. J.; Hu, X.; Lim, K. F.; Lu, D.-H.; Peslherbe, G. H.; Swamy, K. N.; Van de Linde, S. R.; Wang, H.; Wolf, R. J. *Quantum Chemistry Program Exchange Bulletin* **1996**, *16*, 671.
(29) Garcia, E.; Laganà, A.; Sánchez, C. *5th European Conference on Computational Chemistry*, La Londe Les Maures, France, 2004.
(30) Ochoa de Aspuru, G.; Clary, D. C. *XVI Int. Conference on Molecular Energy Transfer*; Assisi, Italy, 1999.
(31) Laganà, A. *J. Chem. Phys.* **1991**, *95*, 2216.
(32) Laganà, A.; Ferraro, G.; Garcia, E.; Gervasi, O.; Ottavi, A. *Chem. Phys.* **1992**, *168*, 341.
(33) Garcia, E.; Laganà, A. *J. Chem. Phys.* **1995**, *103*, 5410.
(34) Laganà, A.; Ochoa de Aspuru, G.; Garcia, E. *J. Chem. Phys.* **1998**, *108*, 3886.
(35) Ochoa de Aspuru, G.; Clary, D. C. *J. Phys. Chem. A* **1998**, *102*, 9631.
(36) Rodríguez, A.; Garcia, E.; Hernández, M. L.; Laganà, A. *Chem. Phys. Lett.* **2002**, *360*, 304.
(37) Garcia, E.; Rodrıguez, A.; Hernández, M. L.; Laganà, A. *J. Phys. Chem. A* **2003**, *107*, 7248.
(38) Garcia, E.; Laganà, A. *Mol. Phys.* **1985**, *56*, 621.
(39) Garcia, E.; Laganà, A. *Mol. Phys.* **1985**, *56*, 629.
(40) Dini, M. *Tesi di Laurea*; Università di Perugia: Perugia, Italy, 1986.
(41) Laganà, A.; Dini, M.; Garcia, E.; Alvariño, J. M.; Paniagua, M. *J. Phys. Chem.* **1991**, *95*, 8379.
(42) Alvariño, J. M.; Hernández, M. L.; Garcia, E.; Laganà, A. *J. Chem. Phys.* **1986**, *84*, 3059.
(43) Laganà, A.; Gervasi, O.; Garcia, E. *Chem. Phys. Lett.* **1988**, *143*, 174.
(44) Palmieri, P.; Garcia, E.; Laganà, A. *J. Chem. Phys.* **1988**, *88*, 181.
(45) Laganà, A.; Hernández, M. L.; Alvariño, J. M.; Castro, L.; Palmieri, P. *Chem. Phys. Lett.* **1993**, *202*, 284.
(46) Laganà, A.; Alvariño, J. M.; Hernández, M. L.; Palmieri, P. Martınez, T.; Garcia, E. *J. Chem. Phys.* **1997**, *106*, 10222.
(47) Aguado, A.; Paniagua, M. *J. Chem. Phys.* **1992**, *96*, 1265.
(48) Aguado, A.; Tablero, C.; Paniagua, M. *Comp. Phys. Comm.* **1998**, *108*, 259.
(49) Aguado, A.; Suárez, C.; Paniagua, M. *J. Chem. Phys.* **1994**, *101*, 4004.
(50) Aguado, A.; Tablero, C.; Paniagua, M. *Comp. Phys. Comm.* **2001**, *134*, 97.
(51) Tablero, C.; Aguado, A.; Paniagua, M. *Comp. Phys. Comm.* **2001**, *140*, 412.
(52) Tablero, C.; Aguado, A.; Paniagua, M. *J. Chem. Phys.* **1999**, *110*, 7796.
(53) Laganà, A. Toward a Grid Based Universal Molecular Simulator. In *Theory of the Dynamics of Elementary Chemical Reactions*; NATO ARW, Laganà, A., Lendvay, G., Eds.; Kluwer: Dordrecht, 2004; p 333.
(54) Faginas Lago, N. PhD Thesis; Università di Perugia: Perugia, Italy, 2002.
(55) Laganà, A.; Crocchianti, S.; Faginas Lago, N.; Pacifici, L.; Ferraro, G. *Collect. Czech. Chem. Commun.* **2003**, *68*, 307.
(56) Laganà, A.; Ochoa de Aspuru, G.; Garcia, E. *J. Phys. Chem.* **2003**, *99*, 17139.
(57) Alagia, M.; Balucani, N.; Casavecchia, P.; Laganà, A.; Ochoa de Aspuru, G.; Van Kleef, E. H.; Volpi, G. G.; Lendvay, G. *Chem. Phys. Lett.* **1996**, *258*, 323.
(58) Laganà, A.; Garcia, E.; Ochoa de Aspuru, G. *Faraday Discuss. Chem. Soc.* **1998**, *110*, 211.
(59) Rodríguez, A.; Garcia, E.; Hernández, M. L.; Laganà, A. *Chem. Phys. Lett.* **2003**, *371*, 223.
(60) Wang, H.; Sun, X.; Miller, W. H. *J. Chem. Phys.* **1998**, *108*, 9726.
(61) Martınez-Núñez, E.; Fernández-Ramos, A.; Vázquez, S. A.; Ríos, M. A. *Chem. Phys. Lett.* **2002**, *360*, 59.
(62) Simpson, W. R.; Rakitzis, T. P.; Kandel, S. A.; Orr-Ewing, A. J.; Zare, R. N. *J. Chem. Phys.* **1995**, *103*, 7313.